MPS/SM/Note 74-2
3 January 1974

MEASUREMENT OF NEW COMPACT OCTUPOLES WITH HARMONIC COIL

A.K. Mitra and F. Rohner

1. INTRODUCTION

The methods of measuring the multiple field coefficients of magnets have been discussed in several publications[1-3]. A number of new compact octupoles have been measured by harmonic field coil method and the field coefficients for different harmonics thus obtained have been used to evaluate different properties of the magnets.

2. THEORY OF MEASUREMENT[4]

Referring to Fig. 1, the wires of the coil are assumed to be concentrated on two radii at the angles v_1 and v_2. The induced flux Φ in the coil will be derived from the flux Φ_ℓ between two wires of length ℓ each, parallel to the S-axis. The flux contribution due to the n^{th} harmonic, in the cylindrical coordinates, is

$$\Phi_{\ell n} = \mu_0 \int \bar{H}\, \overline{ds} = \mu_0\, \ell \int_{v_1}^{v_2} H_r\, r\, d\phi \ . \qquad (1)$$

Assuming

$$B_r = \sum_{n=1}^{\infty} (n\, a_n\, r^{n-1} \sin n\phi + n\, b_n\, r^{n-1} \cos n\phi) \qquad (2)$$

$$\Phi_{\ell n} = 2\, \ell\, r^n\, (a_n \sin n v_0 + b_n \cos n v_0) \sin n\phi \qquad (3)$$

where $v_0 = (v_1 + v_2)/2$ = position of harmonic coil and $\phi = (v_2 - v_1)/2$ = aperture of winding.

To evaluate the flux induced in the coil due to the n^{th} harmonic, Eq. (3) has to be integrated over the area bounded by X_1, X_2, Y_1, Y_2.

$$\Phi_n = 2\, \ell\, (a_n \sin n v_0 + b_n \cos n v_0) \int_{x_1}^{x_2} \int_{y_1}^{y_2} r^n \sin n\phi \, dx\, dy \ , \qquad (4)$$

where $\phi = a \tan (y/x)$, $r = \sqrt{x^2 + y^2}$, in rectangular coordinates.

Introducing a complex variable $z = x + iy$

$$r^n \sin n\phi = \mathrm{Im}\,(z^n) = \mathrm{Im}\,(x + iy)^n$$

$$\Phi n = \frac{-2\,\ell\,\lambda}{(n+1)(n+2)} (a_n \sin n v_0 + b_n \cos n v_0)\ \mathrm{Re}\,(x + iy)^{n+2} \begin{vmatrix} X_2 & Y_2 \\ X_1 & Y_1 \end{vmatrix} \qquad (5)$$

where λ = winding density (number of wires per mm^2).

Through EVLMAG (computer program -- evaluation of field coefficients of magnets), α_n and β_n are obtained for different values of n (harmonics). For an octupole

$$\alpha_n = \frac{n\, a_n\, r_N^{n-1}}{4\, a_4\, r_N^3} \qquad (6)$$

and

$$\beta_n = \frac{n\, b_n\, r_N^{n-1}}{4\, a_4\, r_N^3} \qquad (7)$$

where r_N = normalized radius.

From Eqs. (5), (6), and (7), and after simplification, for n up to 15,

$$\Phi_n = -8\, \ell_{eq}\, \lambda\, r_N^3\, a_4 \sum_{n=1}^{15} \frac{(\sin n v_0 + \cos n v_0)\ \mathrm{Re}\,(x + iy)^{n+2}}{n(n+1)(n+2)\, r_N^{n-1}} \begin{vmatrix} X_2 & Y_2 \\ X_1 & Y_1 \end{vmatrix} \qquad (8)$$

2.1 Octupole effect

From the measurement of flux for a fixed position v_0 and a current I, the octupole effect can be obtained by rearranging Eq. (8):

$$\text{Octupole effect} = \int B''' \, d\ell = 24 \int C_4 \, d\ell = 24 \sqrt{\alpha_4^2 + \beta_4^2} \int a_4 \, d\ell$$

$$= 3 \sqrt{\alpha_4^2 + \beta_4^2}\ \frac{\Phi_{\text{measured}}}{\lambda\, r_N^3 \sum_{n=1}^{15} \alpha_n \dfrac{\sin n v_0 + \beta_n \cos n v_0}{n(n+1)(n+2)\, r_N^{n-1}}\ \mathrm{Re}\,(X + iY)^{n+2} \begin{vmatrix} X_2 & Y_2 \\ X_1 & Y_1 \end{vmatrix}} \qquad (9)$$

For the actual calculation the measured subharmonic coefficients ($n < 4$) have been ignored.

2.2 Effective length (ℓ_{eff})

$$\ell_{eff} = \frac{\int C_4 \, d\ell}{C_4} \tag{10}$$

where $C_4 = \mu_0 NI/a^4$; N = No. of turns/coil of octupole; I = current in the coil; a = radius of the aperture.

2.3 Remanent field

In the absence of current through the magnet, the harmonic coil is rotated from one pole to the next. Let the measured flux be $2\Phi_{rem}$. Assuming no saturation at the measuring current I,

$$\int C_{4rem} \, d\ell = \frac{\Phi_{rem}}{\Phi_{measured}} \int C_4 \, d\ell. \tag{11}$$

$$C_{4rem} = \frac{\int C_{4rem} \, d\ell}{\ell_{eff}} \tag{12}$$

$$B_{rem} \text{ (at 60 mm)} = 4 \, C_{4rem} \, a^3 \tag{13}$$

3. DESIGN PARAMETERS OF THE OCTUPOLE

Physical

Over-all length maximum	280 mm
Iron length	190 mm
Aperture	122 mm
Radius of pole tips	26.5 mm
Weight (approximately)	160 kg

Magnetic

Octupole effect $\int B''' \, d\ell$	2750 Tm^{-2}
Effective length for B	217 mm
Constant K in $B = Kr^3$	2112 Tm^{-3}
Flux density in the pole vertex	4800 G
Maximum flux density in the core	1.2 T
Stored magnetic energy	277 J
Remanent field at r = 4 cm	1.2 G
Integrated field error at x = 5.3 cm	< ±1%

Electrical

Excitation current	646 A
Number of turns per pole	9
Resistance at 60°C	28 mΩ
Inductance at 50 Hz	1.0 mH
Power dissipation	3900 W
Cross-section of conductor	7 × 6.5 mm, Ø 4 mm

Hydraulic

Number of parallel water circuits	2
Temperature rise (r.m.s.)	20°C
Total water flow	3 ℓ/min
Pressure drop	4 atm
Length of one water circuit	23 m
Temperature rise (max.) without water cooling	2°C

4. MEASURING SET-UP

The measuring apparatus used for the CERN Proton Synchrotron Booster magnet has been used. The magnets are pulsed by a BBC power supply. The time sequence of flux and current measurement is shown in Fig. 2. The measuring data is stored on punched cards. The IBM card punch is coupled directly to the remote power supply, the integrating digital voltmeter, the coordinate transducer and a measurement mode encoder. The measurement has been done with a long uncompensated harmonic coil. The harmonic field coefficients are obtained from EVLMAG (the punched cards being the input data for EVLMAG). The flux induced on the harmonic coil for a complete rotation of 360° is shown in Fig. 3.

4.1 Measuring parameters and result

Measuring coil position: $X_1 = 54.0$ mm, $Y_1 = 7.0$ mm,
$X_2 = 57.0$ mm, $Y_2 = 10.04$ mm.

Wire density: $\lambda = 48.8$ windings/mm^2

Normalized radius: $r_N = 60.0$ mm.

Sample measurement: at $I = 493.28$ A, $\Phi_{measured}(v_0 = 25°) = 442.215$ mV sec, and $\Phi_{rem} = 0.259$ mV sec.

Calculated: $\int B''' d\ell = 2136.57$ T/m^2

$\ell_{eff} = 220.0$ mm

B_{rem} (at 60 mm) = 2.0 G.

The measurement, as outlined above, has been done for nine new compact octupoles and the results are summarized in Tables 1 and 2. Figure 4 shows the integrated field $\int B\, d\ell$ measured under a pole for different excitations. With the values of alpha and beta for different n (harmonic) as shown in Table 1, the integrated field and its derivatives are computed and they are shown in Fig. 5.

5. CONCLUSION

The measurements showed that the pole profiles of the octupoles have been well designed to compensate for the 24-pole component of the field. However, the subharmonic coefficients were much higher than expected. This could be due to the misalignment of the measuring system and asymmetry of the octupole (tolerance ±0.1 mm).

* * *

REFERENCES

1) K.D. Lohmann, CERN/SI/Int. MNE/72-1, September, 1972.

2) K.D. Lohmann and C. Iselin, SI/Note MAE/69-18/Rev. 1, 31.7.1970.

3) C. Germain, Nuclear Instrum. Methods 21, 17-46 (1963).

4) M. Gyr, unpublished work on measurement of prototype octupole.

Distribution (open)

MPS/SR/AM

Table 1

Multiple coefficients from EVLMAG

n	‰	New compact octupoles								
		1	2	3	4	5	6	7	8	9
10	alpha	0.26	1.09	0.46	0.95	-0.14	1.48	1.58	0.61	2.66
	beta	-3.22	-3.79	-3.94	-0.22	-2.73	-1.27	-1.48	-1.3	-2.14
12	alpha	-1.16	2.47	3.95	0.22	-0.45	0.06	-0.23	2.43	-0.19
	beta	-0.28	-0.04	0.21	-0.19	-0.24	0.27	0.87	-0.07	-0.12
14	alpha	0.2	0.28	-0.03	-0.05	0.38	0.81	0.17	0.31	1.47
	beta	-0.26	0.77	-0.68	-0.07	0.26	0.07	0.12	-0.32	-0.57
16	alpha	0.03	-0.23	0.9	-0.42	-0.95	-0.72	0.21	0.23	-1.93
	beta	-0.11	0.29	1.43	-0.61	0.08	0.38	0.13	0.67	1.11
18	alpha	0.14	0.13	-1.17	0.93	-0.03	0.2	0.38	-0.04	0.65
	beta	-0.19	-0.09	-1.64	-0.29	-0.17	0.15	0.25	0.16	0.27
20	alpha	0.34	1.95	3.03	0.43	0.24	1.38	0.85	1.11	0.49
	beta	-0.22	-0.69	1.59	-0.07	-0.17	-0.31	-0.06	0.18	0.08
22	alpha	0.17	-0.01	-0.87	-0.22	0.54	0.32	0.16	0.16	0.29
	beta	0.22	-0.61	-1.18	0.19	0.27	0.24	0.41	-0.29	0.02
24	alpha	0.07	0.32	0.94	0.01	-0.51	-0.7	-0.44	-0.3	-1.13
	beta	-0.45	-1.3	2.63	-0.75	-0.14	0.43	0.66	0.4	0.46
26	alpha	0.15	0.11	-0.84	0.1	-0.41	-0.03	0.19	0.12	0.36
	beta	-0.57	-0.14	-1.63	-0.75	-0.93	-0.51	-0.42	-1.15	-0.45
28	alpha	-0.06	1.39	3.43	0.1	0.43	-0.01	0.0	0.87	0.53
	beta	-0.74	-0.08	1.71	0.2	0.0	0.13	0.28	1.04	0.1
30	alpha	0.71	2.61	-3.86	0.17	0.62	0.25	0.26	0.12	0.37
	beta	-0.2	-3.82	-2.68	-0.35	-0.27	-0.31	0.01	-1.27	-0.49

Table 2

Field error, octupole effect, effective length, and remanent field

New compact octupole	Field error at 60 mm ($‰$)	Octupole effect $\int B''' d\ell$ normalized at 600 A (±2%) (T/m^2)	Effective length (±1%) (mm)	Remanent field (r = 60 mm) (G)
1	1.0	2598	221	2.1
2	10.0	2614	222	2.1
3	6.0	2630	224	2.1
4	3.0	2567	218	2.0
5	0.0	2565	218	2.1
6	3.0	2586	220	1.8
7	3.0	2640	224	1.7
8	6.0	2647	225	2.4
9	4.0	2659	226	2.0

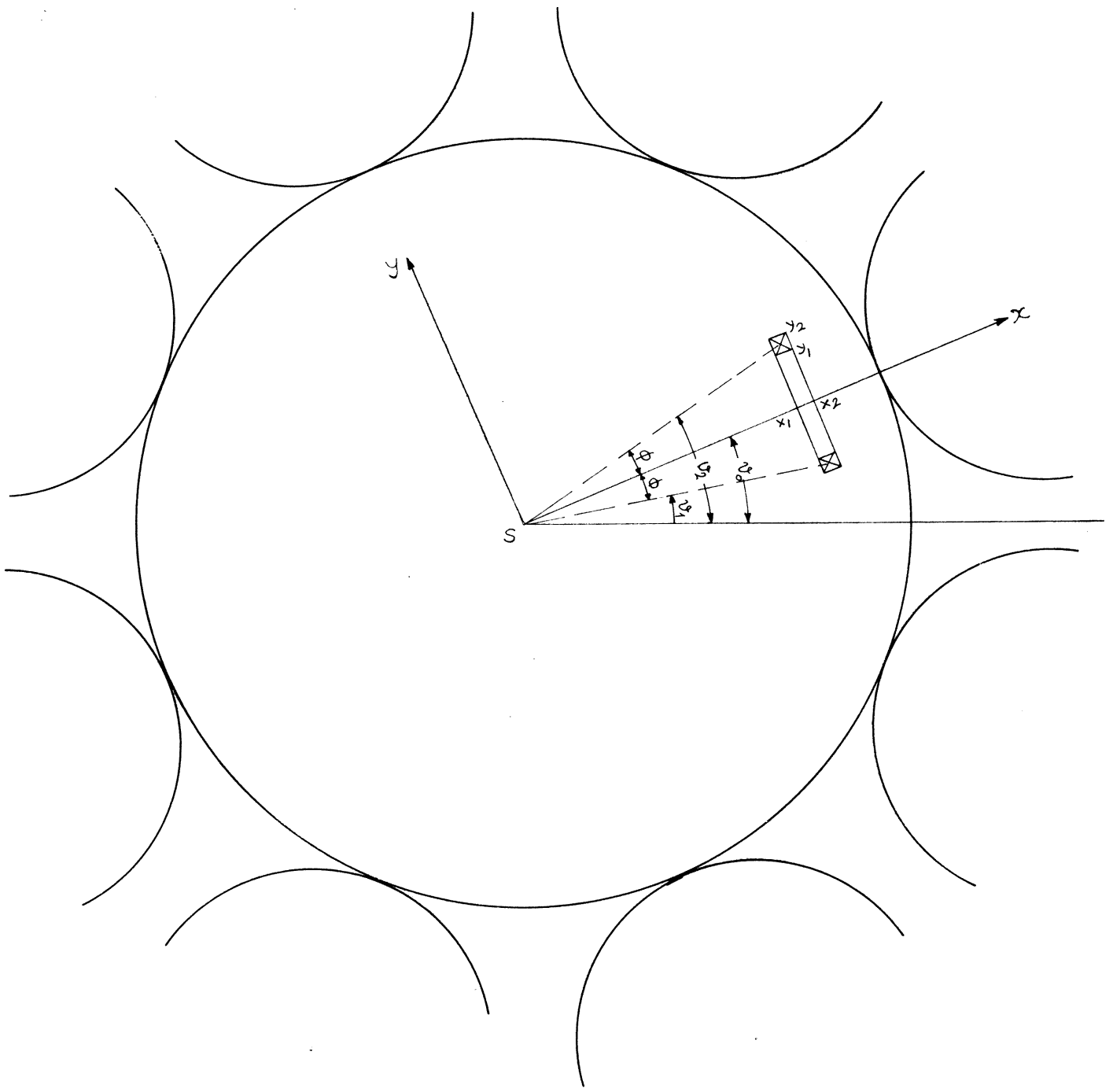

Fig. 1 Coordinate system of the harmonic coil

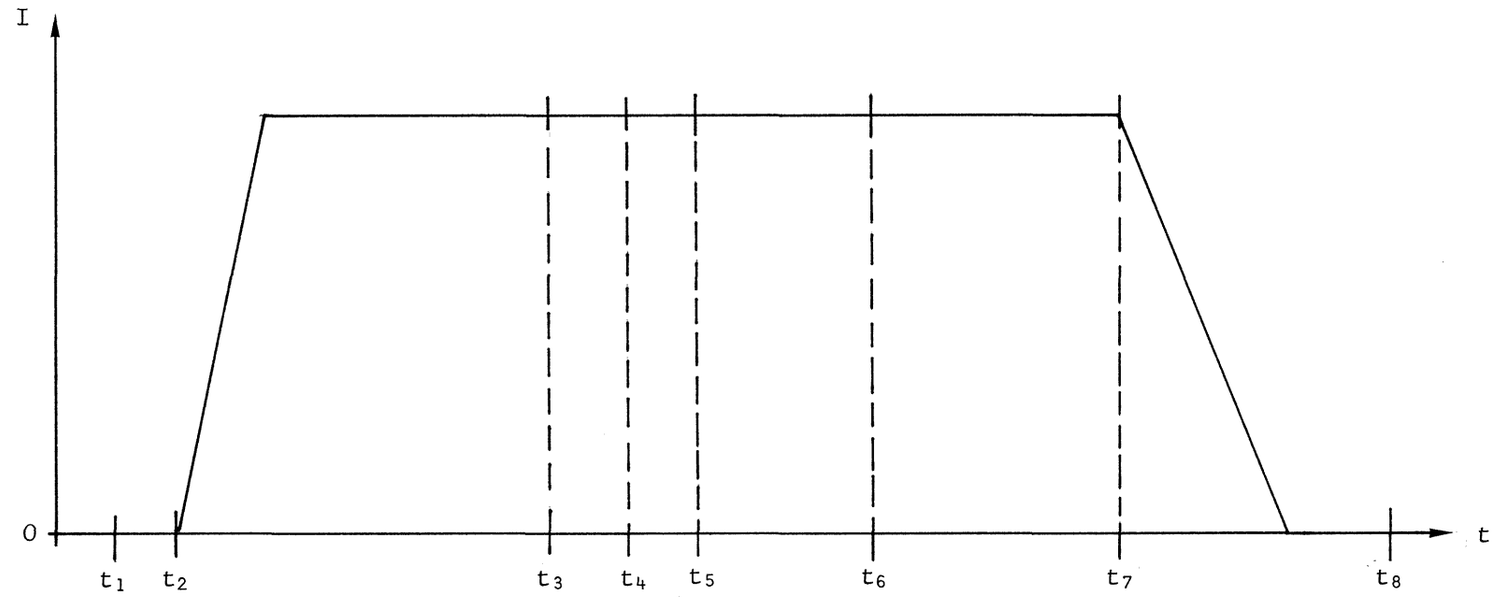

Fig. 2 Scheme of measurement

t_1: flux measure START

t_2: current from power supply START

t_3: current measure START

t_4: flux measure STOP

t_5: current measure STOP

t_6: flux measure RESET

t_7: current from power supply STOP

t_8: current from power supply RESET

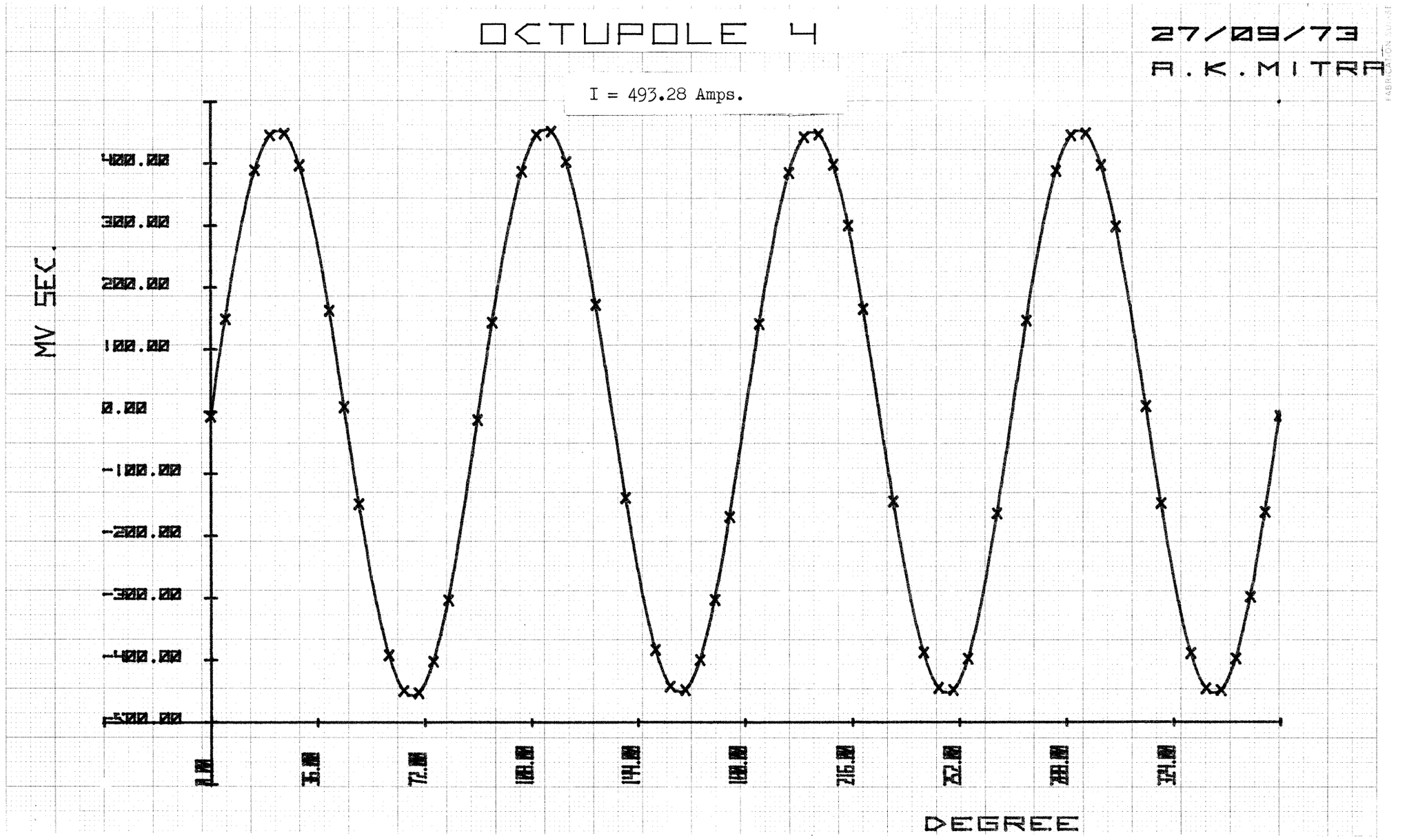

Fig. 3 Flux induced in the harmonic coil

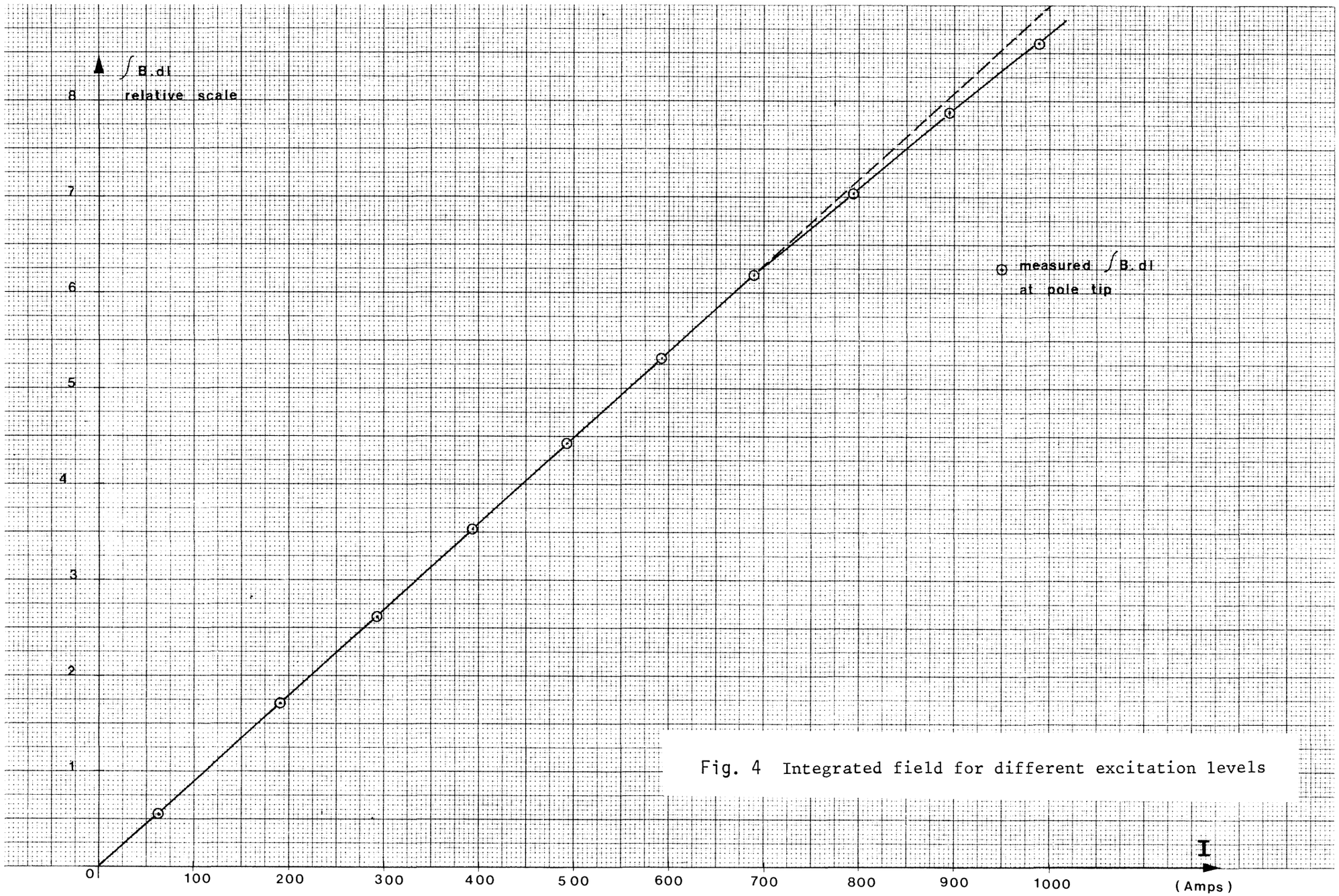

Fig. 4 Integrated field for different excitation levels

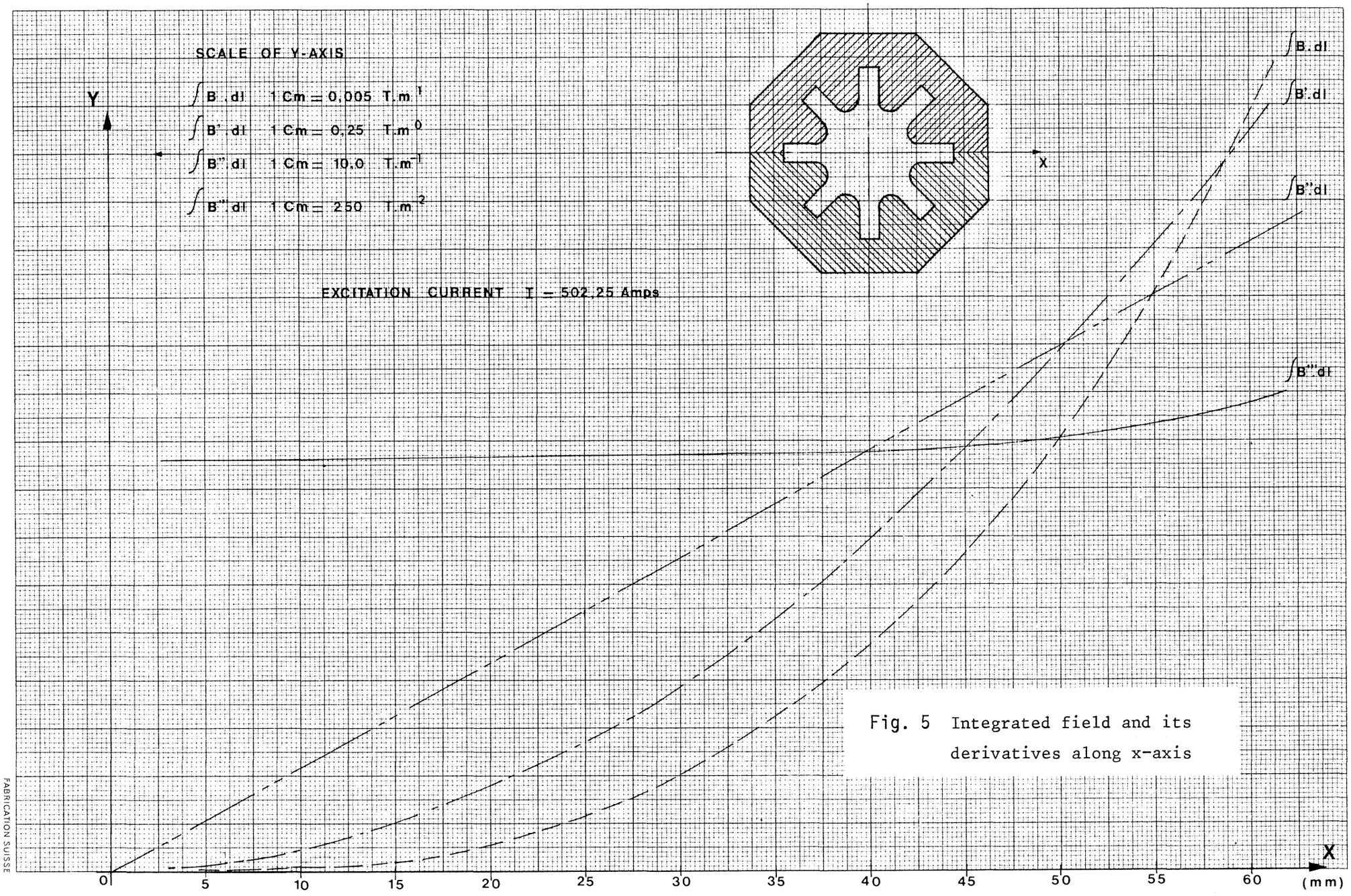

Fig. 5 Integrated field and its derivatives along x-axis